

Article

# Curcumin-Loaded Nanofibrous Matrix Accelerates Fibroblast Cell Proliferation and Enhances Wound Healing via GSK3- $\beta$ Inhibition

Kiran Konain <sup>1</sup>, Nayyer Saddique <sup>1</sup>, Muhammad Samie <sup>2</sup>, Zia Ur Rahman <sup>3</sup>, Sajida Farid <sup>4</sup>, Shazia Hameed <sup>4</sup>, Munazza R. Mirza <sup>5</sup>, Wenhui Wu <sup>6</sup>, Kyung Mi Woo <sup>7</sup>, Praveen R. Arany <sup>8</sup> and Saeed Ur Rahman <sup>4,8,\*</sup>

- <sup>1</sup> Molecular Biology, Institute of Basic Medical Sciences, Khyber Medical University, Peshawar 25100, Pakistan; kiran.konain@hotmail.com (K.K.); nayyersiddique12@gmail.com (N.S.)
- <sup>2</sup> Institute of Pharmaceutical Sciences, Khyber Medical University, Peshawar 25100, Pakistan; sami.jadoon.83@gmail.com
- <sup>3</sup> College of Veterinary Sciences, Faculty of Animal Husbandry and Veterinary Sciences, The University of Agriculture, Peshawar 25100, Pakistan; drzia80@aup.edu.pk
- <sup>4</sup> Oral Biology, Institute of Basic Medical Sciences, Khyber Medical University, Peshawar 25100, Pakistan; drsajidafarid@gmail.com (S.F.); shaziahameed484@gmail.com (S.H.)
- <sup>5</sup> Dr. Panjwani Center for Molecular Medicine and Drug Research, International Center of Chemical and Biological Sciences, University of Karachi, Karachi 75270, Pakistan; munzihyder@yahoo.com
- <sup>6</sup> Department of Marine Bio-Pharmacology, College of Food Science and Technology, Shanghai Ocean University, Shanghai 201306, China; whwu@shou.edu.cn
- <sup>7</sup> Department of Molecular Genetics, Dental Research Institute, School of Dentistry, Seoul National University, Seoul 08826, Republic of Korea; kmwoo@snu.ac.kr
- <sup>8</sup> Oral Biology, Surgery and Biomedical Engineering, University at Buffalo, Buffalo NY 14214-8024, USA; prarany@buffalo.edu
- \* Correspondence: saeed.ibms@kmu.edu.pk or saeedbio80@gmail.com



**Citation:** Konain, K.; Saddique, N.; Samie, M.; Rahman, Z.U.; Farid, S.; Hameed, S.; Mirza, M.R.; Wu, W.; Woo, K.M.; Arany, P.R.; et al. Curcumin-Loaded Nanofibrous Matrix Accelerates Fibroblast Cell Proliferation and Enhances Wound Healing via GSK3- $\beta$  Inhibition. *J. Compos. Sci.* **2023**, *7*, 343. <https://doi.org/10.3390/jcs7080343>

Academic Editor: Francesco Tornabene

Received: 30 June 2023

Revised: 9 August 2023

Accepted: 14 August 2023

Published: 21 August 2023



**Copyright:** © 2023 by the authors. Licensee MDPI, Basel, Switzerland. This article is an open access article distributed under the terms and conditions of the Creative Commons Attribution (CC BY) license (<https://creativecommons.org/licenses/by/4.0/>).

**Abstract:** Wound healing is a multifaceted biological process influenced by both intrinsic and extrinsic factors. The ability of Wnt signaling to activate cell proliferation appears to serve a central role in wound healing. Therefore, the direct activation of Wnt or inhibition of the Wnt antagonist could be an ideal approach for the stimulation of wound healing. This study aimed to investigate the underlying mechanism of small molecule-loaded nanofibrous matrix in inducing wound healing. Herein, a naturally derived small molecule, curcumin, was used to inhibit the GSK3- $\beta$ , which is considered a negative regulator of the Wnt/ $\beta$ -catenin signaling pathway. The docking results demonstrated that curcumin makes a complex with GSK3- $\beta$  at seven specific sites, thereby inhibiting its activity. Moreover, the stabilization of  $\beta$ -catenin appeared to be increased with the treatment of curcumin. Next, curcumin was incorporated in poly  $\epsilon$ -caprolactone nanofibrous matrices for controlled-sustained drug release to induce cell function. Curcumin-loaded nanofibrous matrix not only enhanced fibroblast cell proliferation, but also induced the expression of the fibroblast growth factor (FGF) in vitro. Moreover, the in vivo results showed that these nanofibrous mats significantly induced wound closure in 12 mm critical-sized defect. Collectively, these results suggest that the developed nanofibrous matrix promotes impaired wound healing by modulating cell proliferation and enhancing FGF expression that promotes wound closure.

**Keywords:** curcumin; GSK3- $\beta$ ; poly  $\epsilon$ -caprolactone; nanofibers; wound healing

## 1. Introduction

Wound healing involves complex cellular and molecular interactions that alter cell functions and the dynamic regulation of extracellular matrices to modulate tissue repair and regeneration [1]. Disruption of any of these factors can delay the healing process, leading to the development of chronic wounds. Extensive research has been carried out over the past three decades on wound repair and regeneration. The current conventional

treatment includes bleeding control, use of systemic or topical antibiotics and wound disinfectants, and dressings [2]. It has been suggested that the antimicrobial efficacy of advanced dressing alone is inadequate, and other niches with enhanced wound healing potential are desirable [3,4]. However, current treatments involving growth factors and other biologicals are still inadequate, time-consuming, and costly/expensive.

Wound dressings have evolved from simple physical covering to sophisticated drug delivery systems. Both natural and synthetic polymers are being utilized depending on the type of damaged tissue. Synthetic polymer scaffolds in this regard have some distinct advantages over natural polymer scaffolds, such as controlled fiber diameter, non-immunogenicity, and ease of fabrication [5]. These scaffolds have been fabricated in various forms, such as nanofibers, nanoparticles, gels, and microspheres. Among these, nanofibrous matrices are receiving significant attention for various biomedical applications, as they mimic natural collagen fibrils present in the extracellular matrix microenvironment [6,7]. The nanotopology and surface-to-volume ratio of the nanofiber matrix reveal essential properties for increased interaction with the cells and tissue, thereby providing an ideal substrate for the controlled and sustained delivery of bioactive molecules that target specific wound signaling pathways [8,9].

Cell signaling pathways are the central pillars in wound repair and regeneration, including the FGF/TGF- $\beta$  and Wnt/ $\beta$ -catenin pathways. A disrupted release of these molecules can affect fibroblast cell function and wound repair. Among them, the Wnt/ $\beta$ -catenin pathway plays key roles in cell proliferation in wound healing [10,11]. The most important signaling intermediate in this pathway is the GSK3- $\beta$  enzyme, which causes the phosphorylation and degradation of the  $\beta$ -catenin protein. The inhibition of GSK3- $\beta$  results in  $\beta$ -catenin activation and translocation into the nucleus to regulate the gene expression. Previous studies using several animal models suggest that small molecules such as glycogen synthase kinase 3- $\beta$  (GSK3- $\beta$ ) inhibitors are effective agents for promoting the wound healing process [12].

One of the major natural small molecules is curcumin (Cur), which is known to inactivate GSK3- $\beta$ , thus promoting Wnt/ $\beta$ -catenin signaling to enhance wound healing [12]. The pharmacological and biological efficacy of Cur is well known as it exhibits anti-infective, anti-inflammatory, and antioxidant properties [13]. Both in vitro and in vivo studies have noted the efficacy of Cur to modulate inflammatory cytokines and increase growth factors [14]. Moreover, the antioxidant ability of Cur to protect keratinocytes and fibroblasts and accelerate wound healing ability in a rat model has been demonstrated [15]. Despite having these distinct biological functions, the in vivo bioavailability and stability of Cur is very low, and its systemic administration is unlikely to provide a significant concentration for cutaneous wound healing. Herein, we investigated curcumin-incorporated nanofibrous matrix fabricated via electrospinning, and its ability to modulate fibroblast function and wound healing was investigated using in vitro and in vivo models. Using in silico modeling, we first examined the ability of Cur to bind GSK3- $\beta$  to modulate Wnt/ $\beta$ -catenin signaling. Then, we investigated the effects of Cur in vitro on fibroblast proliferation and FGF secretion. Finally, we assessed the in vivo efficacy of the Cur-loaded matrix on cutaneous wound healing of a critical-size defect in a rat model.

## 2. Materials and Methods

### 2.1. Molecular Docking

The docking study was performed on curcumin with the target enzyme GSK3- $\beta$ , for which the 3D structure (PDB id = 1PYX) was retrieved from the Protein Data Bank [16]. The amino acids involved in the ATP-binding active pocket of the target were identified from previous literature [17]. Before performing the docking analysis, structure refinement was carried out using ModeRefiner [16]. Patch Dock was used for the molecular docking of the target enzyme and curcumin [18]. The ligand and targeted protein were uploaded in a PDB format. Molecular visualization and analysis of the docked compounds were achieved using the BIOVIA Discovery Studio visualizer 2017R2.

## 2.2. Cell Culture and Viability

A mouse fibroblast cell line, NIH3T3, was procured from IRCBM, COMSATS University Islamabad, and seeded in culture flasks and grown in Dulbecco's Modified Eagle Medium (DMEM) containing 10% FBS and 1% penicillin–streptomycin antibiotics. The cells were seeded in a 24-well plate at a density of  $2 \times 10^4$  cells per well. Following attachment, treatments with Cur at 0, 0.1, 1, and 10  $\mu\text{g}$  per mL were performed. Cell proliferation was assessed after 24 h of incubation using Alamar Blue.

## 2.3. Western Blot Analysis

NIH3T3 cells were seeded at a density of  $5 \times 10^4$  cells per well using a 6-well plate. The cells were harvested and lysed using a lysis buffer containing Triton X-100 and protease inhibitors. Equal amounts of samples were loaded on SDS-PAGE (10–12%) and transferred onto a polyvinylidene difluoride membrane. The membranes were blocked using 1% fetal bovine serum in a TBST buffer (10 mM Tris–HCl, 100 mM NaCl, 0.1% Tween-20) for 1 h at room temperature. Primary antibody ( $\beta$ -catenin, Cell Signaling, 1:1000) was incubated overnight followed by HRP-conjugated secondary antibody (1:10,000 dilutions) the following day for 1 h. Detection was performed using enhanced chemiluminescence (Bio-Image Analyzer).  $\beta$ -actin was used as an internal control. For quantification, blots of the experiments were digitally analyzed via densitometry (NIH ImageJ 1.8.0 software).

## 2.4. Electrospinning

Electrospinning was carried out as described previously using a uniaxial setup (Foshan Nanofiberlabs, Guangdong, China) [6,9,19]. A homogeneous solution of 10% *w/v* was made using PCL beads dissolved in chloroform and dimethylformamide (Sigma Aldrich, St. Louis, MO, USA) in an equal ratio. To generate it, Cur was added to a PCL solution at 0.1, 1, and 5% *w/v*. Syringes (10 cc) with blunt-end needles were used to load the solutions. An aluminum foil-covered rotating collection drum was placed at a distance of 15 cm from the needle, and the rate of solution flow was set to 0.5 mL per hour, and the voltage was adjusted to 17 kV. The electrospinning was continued for 4.5 h to fabricate a  $10 \times 18$  cm sheet of nanofibers.

## 2.5. Morphological Analysis via Scanning Electron Microscopy

Morphological and topographical analyses of the electrospun nanofiber matrices were performed via scanning electron microscopy (SEM) (VEGA 3, TESCAN, Brno, Czech Republic). The samples were subjected to sputter-coating with gold at 15 mA for 90 s. Images were captured with an accelerating voltage of 10 kV, and a 5  $\mu\text{A}$  current was used to observe the samples. The diameter of the electrospun fibers was quantified using the NIH ImageJ software.

## 2.6. FTIR Instrumentation

Fourier transform infrared (FTIR) analysis was performed on Cur, PCLF, and PCLF–Cur nanofibers with Thermo-Nicolet 6700P (Thermo Nicolet Corp., Madison, WI, USA) using an attenuated total reflection FTIR (ATR–FTIR) mode. Continuous scans (128) in the  $650\text{--}4000\text{ cm}^{-1}$  frequency range with a resolution of  $8\text{ cm}^{-1}$  were evaluated using Origin-Lab software (Origin Lab Corporation, Northampton, MA, USA).

## 2.7. Drug Release Study

Nanofiber matrices were cut into  $2 \times 2$  cm pieces with an equal weight of 15 mg, and immersed in 2 mL of phosphate buffer saline (PBS) in 15 mL falcon tubes. Sample incubation was carried out at  $37\text{ }^\circ\text{C}$ . Of the supernatant, 300  $\mu\text{L}$  was collected from each respective tube at 1, 3, 6, 12, 24, and 48 h time intervals, and the absorbance spectrum in triplicate was determined employing UV spectrophotometer to assess the mean cumulative percentage of drug release.

### 2.8. Effect of PCLF–Cur on Cell Viability

PCLF containing varying amounts of Cur nanofiber matrices were placed in a 24-well tissue culture plate. Sample sterilization was performed by UV light for 1 h and incubated overnight with  $2 \times 10^4$  fibroblast cells per well for 24 h. Cell proliferation was assessed with an Alamar Blue assay and spectrophotometry at 550/620 nm. All the samples were used in triplicate and the assay was repeated at least thrice.

### 2.9. FGF ELISA

FGF secretion from fibroblast cells in response to a Cur-containing scaffolds was assessed with an ELISA (PeproTech, London, UK), as per the manufacturer's instructions. Briefly, 96-well plates were coated with FGF-specific antibody overnight and unbound antibodies were removed by washing. Following blocking, recombinant FGF for the standard curve or samples was incubated, followed by detection antibody, amplification, and substrate solution that was detected via absorbance.

### 2.10. Wound Healing Studies in Rodents

All in vivo studies were approved (Dir/KMU-EB/CI/000215) by the animal use and care committee, Khyber Medical University. Male 6-week Sprague-Dawley (SD) rats were procured from NIH (Islamabad, Pakistan). The rats were maintained in a temperature-controlled room ( $25 \pm 1$  °C) with a set 12 h light–dark cycle, chow, and water ad libitum. Wound healing assays were performed on animals, as described previously [20]. Each animal (8 weeks old) was weighed before the study and they ranged between 300 to 350 g. Fifteen male rats were randomly divided into three groups (controls, PCLF, and PCLF–Cur 1% w/v,  $n = 5$  each). The dorsum of each rat was shaved, and 12 mm diameter full-thickness wounds were created using a punch at either side of the dorsal midline. Post-surgery images were taken using a digital camera on days 0 and 9, and quantification of the wound surface was performed using NIH ImageJ, where the wound closure rate was defined as  $\text{Wound Area}_{\text{Day0}} - \text{Wound Area}_{\text{Day9}} / \text{Wound Area}_{\text{Day0}}$ .

### 2.11. Statistical Analysis

Data were analyzed from the representative experiments using Excel (Microsoft 2016, USA). A one-way ANOVA or Student's *t*-tests was used to assess statistical significance, where  $p < 0.05$  was considered statistically significant. The assays were performed in triplicate, and all the studies were repeated at least twice.

## 3. Results

### 3.1. Molecular Interactions between Curcumin and GSK3- $\beta$

Docking analysis was performed to determine putative molecular interactions between curcumin and GSK3- $\beta$  that indicated it could form complexes with GSK3- $\beta$  at specific sites, thereby inhibiting its activity [21]. Curcumin has been noted to bind to the ATP-binding pocket of GSK3- $\beta$  and is considered an ATP-competitive inhibitor. The molecular docking results in this study confirmed that curcumin binds to GSK3- $\beta$  at positions ASP181 and ASP200 via hydrogen bonds, and at CYS199, LEU188, ILE62, ALA83, and VAL70 via van der Waals interactions (Figure 1a,b). These findings revealed that curcumin can inactivate GSK3- $\beta$  which has a key role in the Wnt pathway that is crucial for wound healing.

### 3.2. Stabilization of $\beta$ -Catenin by Curcumin

Next, we examined the effect of curcumin on Wnt/ $\beta$ -catenin signaling.  $\beta$ -catenin is a direct target of GSK-3 $\beta$  and an important mediator of Wnt signaling. It is also involved in the regulation of the transcription of genes associated with cell proliferation and differentiation that are key processes in wound healing [6]. We examined the amounts of  $\beta$ -catenin via Western blots in fibroblasts treated with curcumin. Our study demonstrated that the amount of  $\beta$ -catenin protein was higher in cells treated with curcumin compared

with untreated controls (Figure 2a). Overall, these results establish that curcumin inhibits GSK-3 $\beta$ , leading to the activation and stabilization of  $\beta$ -catenin.

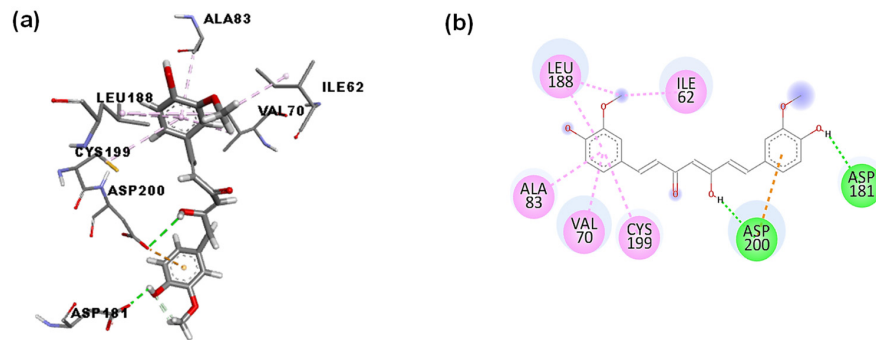


**Figure 1.** Molecular docking showing the interaction between Cur and the amino acids of GSK3- $\beta$  in a (a) 3D and (b) 2D structure.

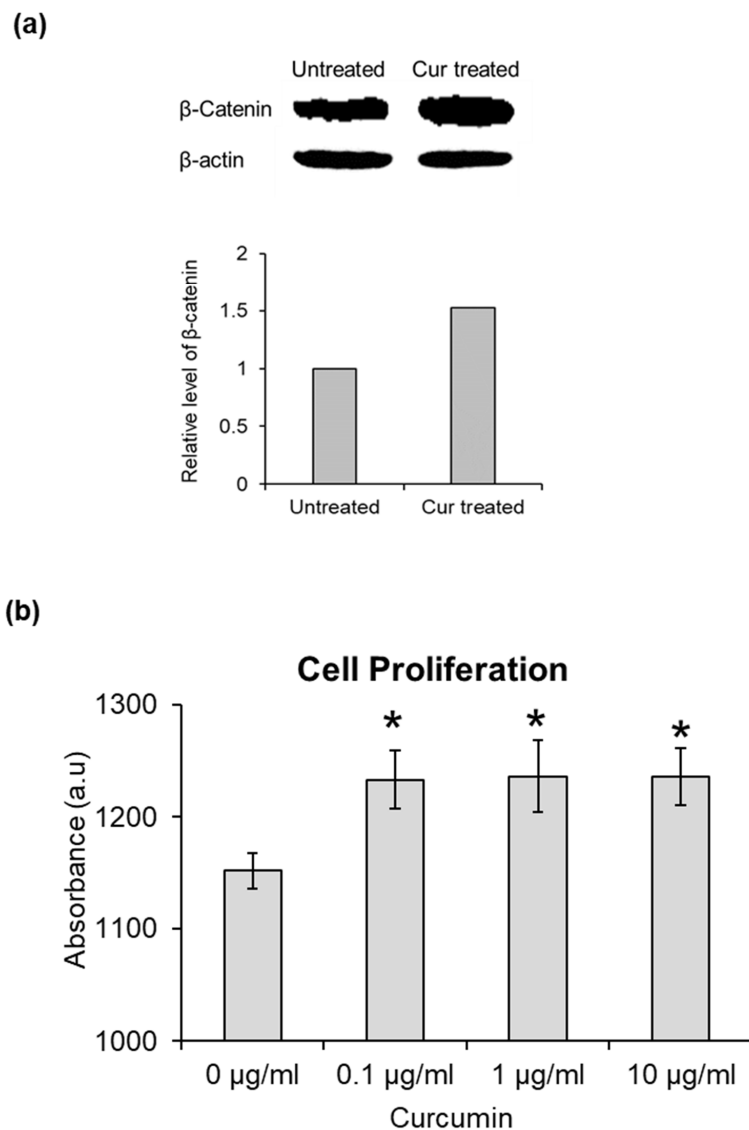


**Figure 2.** (a) Qualitative and quantitative measurements of Western blot results showing significant difference of the  $\beta$ -catenin protein level between untreated and Cur-treated samples. (b) Quantitative cell proliferation assay of fibroblasts cultured with or without Cur treatment at different concentrations. \* significantly ( $p < 0.05$ ) different from the control (0  $\mu$ g/mL).

### 3.3. Effect of Curcumin on Cell Proliferation

Curcumin is an ideal natural candidate for inducing rapid wound healing by stimulating fibroblast cell proliferation and migration [15,22]. The cells were cultured and treated with different concentrations of curcumin, namely, 0.1, 1, and 10  $\mu\text{g}/\text{mL}$  compared to the control (blank). The results showed that curcumin treatment significantly ( $p < 0.05$ ) enhanced cell proliferation compared to control (Figure 2b). However, there were no significant differences in the proliferative response to different concentrations. These findings are consistent with the previous findings that curcumin at a concentration of up to 10  $\mu\text{M}$  (36.8  $\mu\text{g}/\text{mL}$ ) is effective in normal dermal fibroblasts [23]. Higher doses are known to be toxic and thus, we limited our further analysis to these dose ranges.

### 3.4. Morphological Characteristics of Nanofiber Scaffolds

Next, we generated the polymeric scaffold using electrospinning. It is well established that the fiber diameter can be affected by factors such as polymer concentration, conductivity, molecular weight, tip-to-collector distance, humidity, and temperature [24]. We performed SEM analysis to evaluate the difference in surface topography altered by the addition of curcumin. At constant electrospinning conditions, the synthesized nanofiber matrices, i.e., PCLF, PCLF–Cur 0.1, PCLF–Cur 1, and PCLF–Cur 5, were found in the nanometer range with prominent 400–600 nm diameter fibers (Figure 3). The ratios of the nanofibers within the range of 400–600 nm were 37%, 40%, 47%, and 42% for PCLF, PCLF–Cur 0.1, PCLF–Cur 1, and PCLF–Cur 5, respectively. Moreover, our results revealed that the percentage frequency was shifted from a lower (200–400 nm) to higher range (600–800 nm) with increased curcumin concentrations. This increase in nanofiber diameter might be attributed to an increase in solution viscosity caused by the incorporation of curcumin [25]. Overall, our results demonstrated that the fibers were smooth, without any clumps or beads, and uniformly distributed in a 3D fashion that fulfills essential attributes for cell responses.

### 3.5. Confirmation of Curcumin Incorporation in Nanofiber Scaffolds

To determine the successful incorporation of curcumin within the PCLF nanofibers and potential chemical interactions, we performed FTIR analysis. The FTIR spectra of the unloaded curcumin and blank PCLF were also recorded for comparison. We observed specific peaks for curcumin, e.g., C=C stretching vibrations due to the presence of aromatic moieties and a benzene ring, which exhibited a broader peak around  $1630\text{ cm}^{-1}$  (Figure 4). These peaks were evident in the PCLF–Cur scaffolds. Another peak pointing at  $1510\text{ cm}^{-1}$  represents C=O vibrations due to the overlap of the ethylene group. A sharp peak representing the C–O elongation of the hydroxyl group and olefinic C–H bending vibrations appeared at  $1430\text{ cm}^{-1}$ , which has been shortened and broadened in the PCLF–Cur spectra. Two other peaks, i.e., a sharp projection at  $1240\text{ cm}^{-1}$  and a hump-shaped peak at  $1280\text{ cm}^{-1}$ , can also be seen in Cur due to the asymmetric C–O–C stretching vibrations of the ether group. Overall, these results confirmed that Cur has been successfully incorporated into the PCLF, and these were either physical or weak chemical interactions.

### 3.6. Controlled and Sustained Release of Curcumin from PCLF Scaffolds

Previous studies have suggested that bioactive molecules can be added to synthetic bioengineered scaffold systems to support tissue regeneration through the controlled and/or sustained release of drugs at the local defect site [26]. Therefore, in the current study, we sought to engineer curcumin-incorporated PCLF scaffold systems for local drug delivery to enhance wound healing. The cumulative release profile of PCLF–Cur 5 showed the highest release of 32  $\mu\text{g}$  (3.2%  $w/v$ ) after 48 h (Figure 5). Moreover, the release pattern showed a constantly increasing trend of 6.4%, 9.9%, 12.4%, 14.9%, and 17.6% over the periods of 3, 6, 12, 24, and 48 h, respectively. Similarly, the highest release of curcumin from PCLF–Cur 1 was 2.0% at 1 h and constantly increased up to 7.4% at the 48 h time point. The minimum release profile was found in PCLF–Cur 0.1, where 1.2% release was seen after

1 h, and by the end of 48 h, it increased to 4.8%. Overall, these results demonstrated that we both sustained and controlled local curcumin release from the nanofibrous scaffolds were achieved.

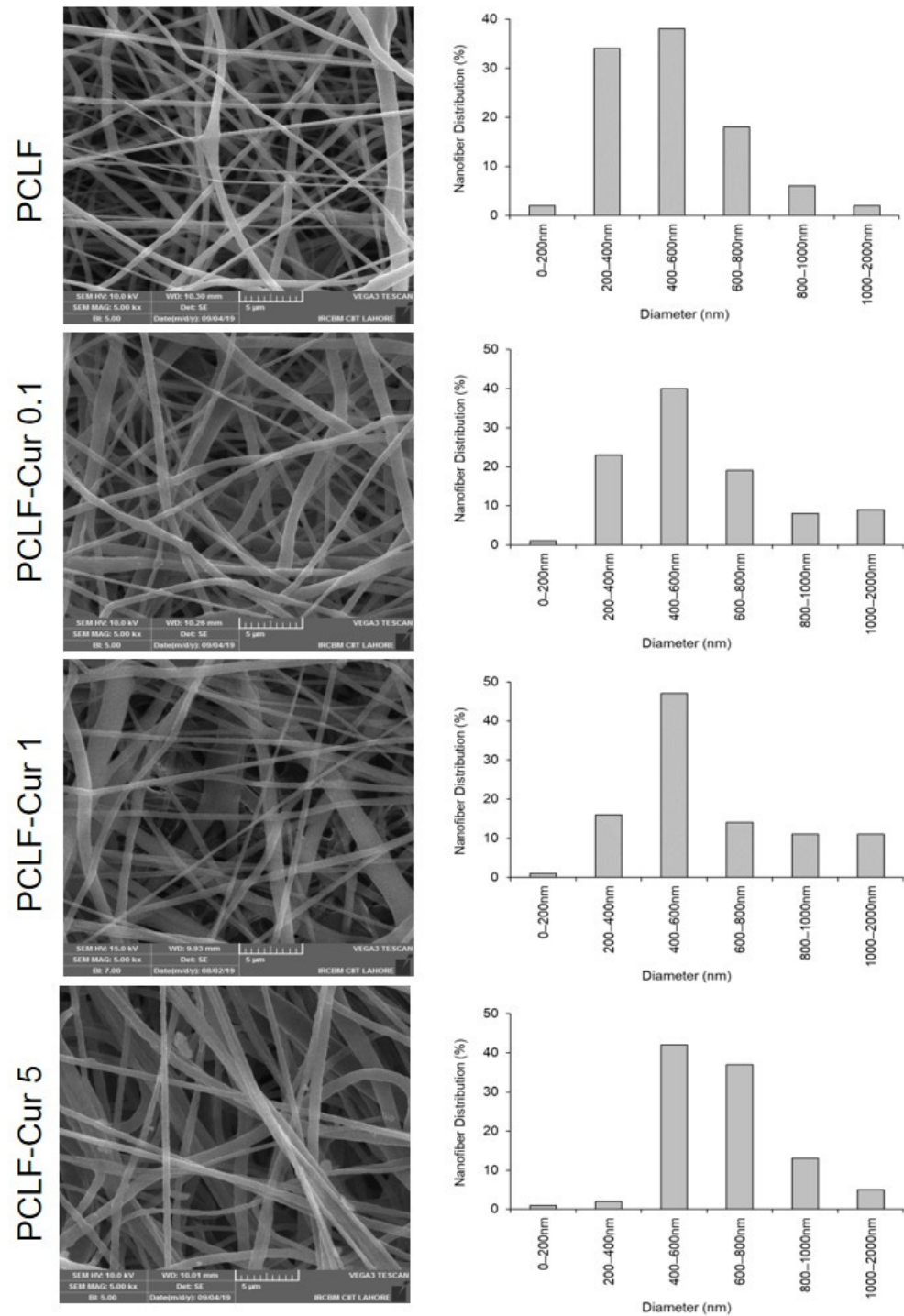


**Figure 3.** Characterization of electrospun nanofibers synthesized from poly  $\epsilon$ -caprolactone (PCL) via electrospinning. SEM images and quantitative analysis of the fiber diameters of PCLF, PCLF-Cur 0.1, PCLF-Cur 1, and PCLF-Cur 5.

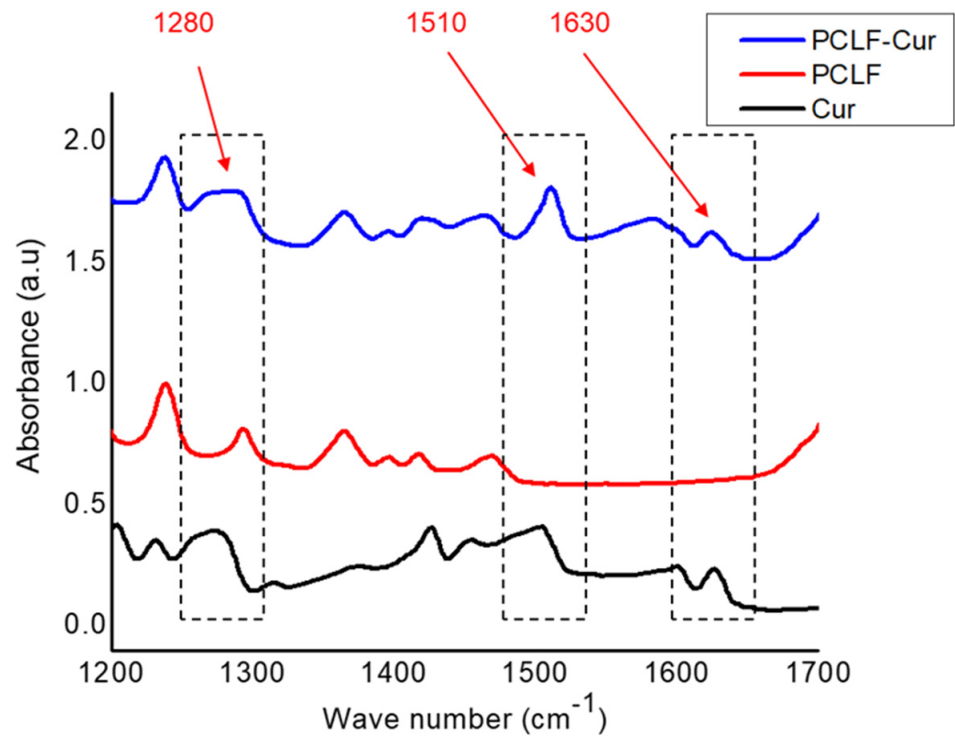


Figure 4. FTIR analysis of Cur, electrospun PCLF, and PCLF–Cur nanofibers.

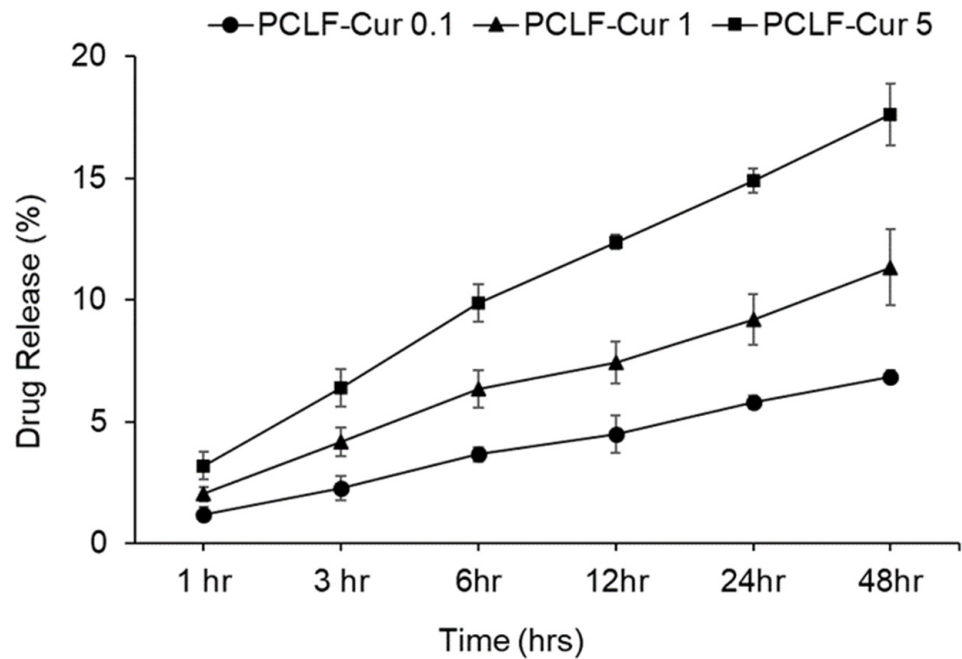
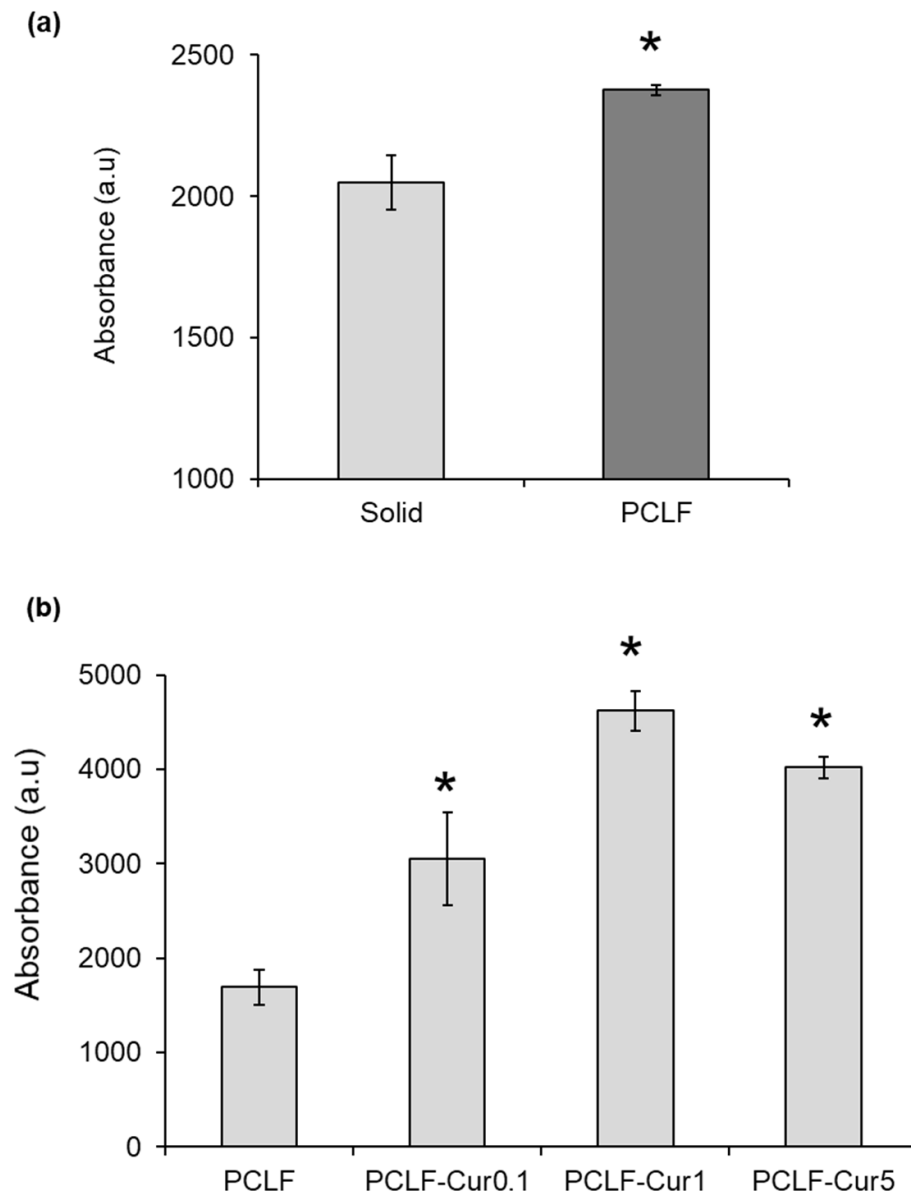


Figure 5. Cumulative percent drug release of Cur from PCLF–Cur 0.1, PCLF–Cur 1, and PCLF–Cur 5 compared with PCLF after 1 h, 3 h, 6 h, 12 h, 24 h, and 48 h. Data area presented as the mean  $\pm$  SD.

### 3.7. Effect of Curcumin-Incorporated Nanofibers on Cell Proliferation

Next, we investigated the *in vitro* cellular responses of curcumin-loaded PCLF scaffolds to fibroblast cells using the Alamar Blue assay. As shown in Figure 6a, PCLF significantly ( $p < 0.05$ ) induced cell proliferation compared to solid PCL. This indicates that the environment provided by the nanoarchitecture of PCLF is an ideal substrate to promote cell proliferation in wound healing. We observed that the cell-proliferative response was further significantly ( $p < 0.05$ ) increased with the addition of curcumin to these PCLF scaffolds.

folds (Figure 6b). Among the curcumin-loaded scaffolds, PCLF–Cur 1 showed the highest proliferation. This may be due to morphological changes in the nanofibers observed with increasing the concentration of curcumin, as noted with fiber diameter distribution. These results suggest that PCLF–Cur 1 would be most suitable for wound healing applications and was therefore chosen for in vivo studies.



**Figure 6.** Proliferation assay of NIH3T3 cells cultured on (a) TCD and PCLF. (b) Quantitative measurement of cell proliferation cultured on PCLF, PCLF–Cur 0.1, PCLF–Cur 1, and PCLF–Cur 5. Data area presented as the mean  $\pm$  SD. \* significantly different from the control ( $p < 0.05$ ).

### 3.8. Biomimetic Nanofibrous Scaffolds on Fibroblast Growth Factor Expression

Next, we determined FGF concentrations in cells cultured on PCLF and PCLF–Cur, as it is a key mitogen for fibroblast cell proliferation [27,28]. We observed that a significant amount of FGF in cells cultured in a nanofibrous environment were significantly ( $p < 0.05$ ) increased as compared to both solid PCL and PCLF controls (Figure 7). Overall, these results suggest that curcumin-incorporated, electrospun nanofibrous scaffolds are an attractive option as wound healing dressing, as they can promote FGF expression and fibroblast proliferation.

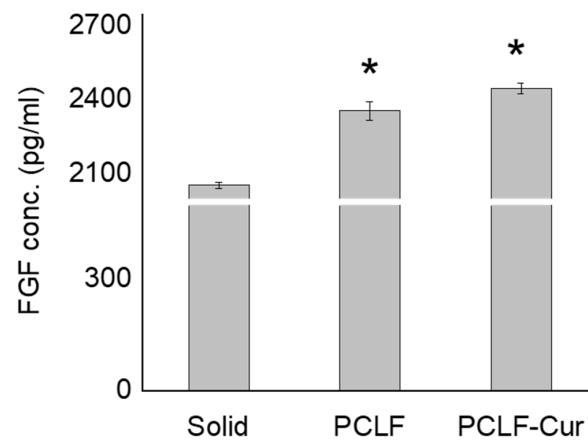


**Figure 7.** NIH3T3 cells cultured on solid (TCD), PCLF, and PCLF-Cur. ELISA results showing the amount of FGF proteins secreted by NIH3T3 cells. Data area presented as the mean  $\pm$  SD. \* significantly different from the control ( $p < 0.05$ ).

### 3.9. PCLF-Curcumin Scaffold for Wound Closure in Rats

Finally, we examined the in vivo effect of PCLF-Cur on mechanically induced full-thickness excisional (12 mm) skin wounds in male rats [20]. The PCLF-Cur accelerated and promoted wound closure with significant differences ( $p < 0.05$ ) compared to the PCLF or untreated controls (Figure 8a). On day 09, the PCLF groups achieved 68% wound closure compared to 64% achieved in control rats, that was not statistically significant. However, the PCLF-Cur group achieved greater-than-80% wound closure (Figure 8b). Overall, these results demonstrated that Cur-incorporated nanofibrous scaffolds can accelerate wound healing.

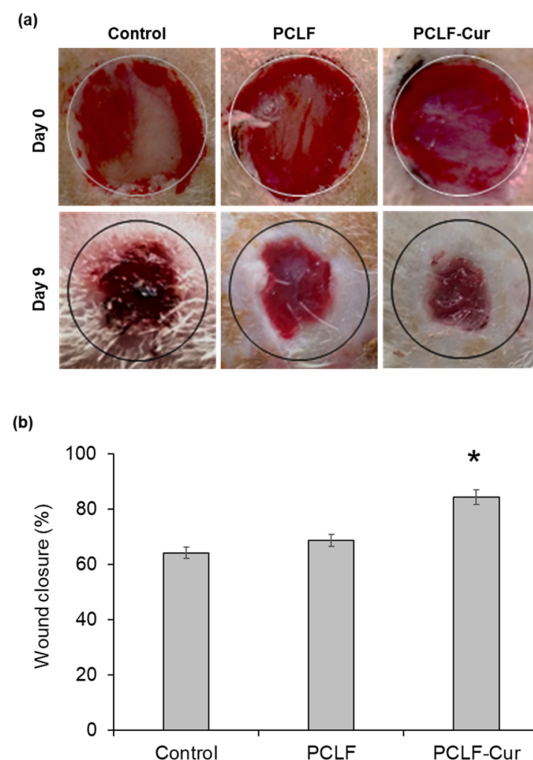


**Figure 8.** Effect of PCLF-Cur on wound closure. (a) Representative digital images of cutaneous wounds on days 0 and 9 post-surgery of control, PCLF and PCLF-Cur groups. (b) Quantitative measurement of wound closure area presented as the mean  $\pm$  SD. \* significant differences between the control or PCLF and PCLF-Cur groups ( $p < 0.05$ ).

#### 4. Discussion

Naturally derived bioactive molecules play a major role in enhancing tissue regeneration and wound healing through multifaceted approaches. Cur is a well-known natural active compound found in turmeric, with diverse biological properties. It has been demonstrated to have anti-inflammatory, anti-bacterial, anti-fungal, anti-oxidant, anti-proliferative, anti-viral, and pro-apoptotic properties, making it useful in a wide variety of disorders [29,30]. Cur is considered an attractive therapeutic molecule due to its minimal toxicity and, at high dosage, exhibits anti-cancer properties [30,31]. Herein, this study explored curcumin-induced fibroblast cell function and wound healing via GSK3- $\beta$  inactivation and potentially inducing Wnt signaling. Our results demonstrated that Cur binds with GSK-3 $\beta$  at seven different binding sites and is capable of inactivating its function. Thus, the results showed stabilization of  $\beta$ -catenin and activation of Wnt signaling.

It is well known that cutaneous wound healing requires the coordination of several types of cells. Among these, fibroblasts are the major contributors that are attracted to the wound site after injury to start proliferation, induce epithelial closure via paracrine signaling, and ECM formation [1,22]. Thus, approaches to accelerate fibroblast functions via bioactive molecules could potentially promote wound healing [32]. Moreover, the fibroblast growth factor (FGF) is also an important mediator for wound healing because it activates the vascular epithelial and fibroblast cells that surround the defect site [33]. Previous studies have reported on the positive feedback mechanism of Wnt and FGF signaling in skin fibroblast cells, as both these pathways contribute to cell function and increased collagen deposition. Knockdown of  $\beta$ -catenin in fibroblasts led to the repression of FGF [34]. In another study, it was reported that bFGF induced wound healing in diabetic animal models by regulating the inflammatory response and re-epithelialization [35]. In the current study, we found that the FGF was highly increased in cells cultured on PCL–Cur scaffolds, correlated with increased fibroblast proliferation.

The extracellular matrix (ECM), a major component of cutaneous tissue, is constantly remodeled to support cell and tissue morphogenesis [34]. The physical properties and molecular composition of ECMs determine the fate and performance of cells while facilitating intercellular communication through the conduction of molecular signals [36,37]. The engineered nanofibrous matrix, which mimics the natural ECM, is an ideal candidate for tissue repair and regeneration. Therefore, in the current study, we developed scaffolds that not only provide structural support, but also released Cur in a precise and regulated manner. The well-known characteristics associated with Cur include improved neovascularization; re-epithelialization; increased migration of various cells, including dermal fibroblasts, myofibroblasts, and macrophages into the wound bed; higher collagen content; and granulation tissue formation [38–40]. We successfully incorporated Cur into PCLF scaffolds through the electrospinning process. No clumping that could lead to bead formation was seen on the nanofiber surface, which shows that the drug was uniformly distributed within the polymer bed. We finally examined that the utility of these PCLF–Cur scaffolds in wound healing was validated using *in vivo* soft tissue wounds in rats. These scaffolds demonstrated significant promotion of a 12 mm excisional skin wound, with over 84% healing.

#### 5. Conclusions

In this study, a biodegradable and biocompatible PCLF electrospun nanofiber with curcumin was fabricated, and its potential utility as therapeutic wound dressing was evaluated. These scaffolds demonstrated a smooth and uniform distribution, along with a controlled and sustained release of curcumin. These curcumin-incorporated nanofibers successfully increased fibroblast proliferation and FGF release *in vitro*, as well as the rate of wound closure in the *in vivo* wound model. Given the non-toxic, affordable, and readily available materials, PCLF–Cur scaffolds should be evaluated in controlled human studies as alternatives to conventional wound dressings.

**Author Contributions:** Conceptualization, K.K. and S.U.R.; Methodology, K.K., N.S. and M.S.; Validation, Z.U.R. and S.U.R.; Formal analysis, M.S. and S.U.R.; Resources, K.K.; Data curation, S.F. and S.H.; Writing—preparation of original version, K.K. and S.U.R.; Writing—reviewing and editing, M.R.M., W.W., K.M.W. and P.R.A.; Supervision, S.U.R. All authors have read and agreed to the published version of the manuscript.

**Funding:** This research received no external funding.

**Data Availability Statement:** The data presented in this study are available on request from the corresponding author.

**Conflicts of Interest:** The authors declare no conflict of interest.

## References

1. Wilkinson, H.N.; Hardman, M.J. Wound healing: Cellular mechanisms and pathological outcomes. *Open Biol.* **2020**, *10*, 200223. [[CrossRef](#)]
2. Monika, P.; Chandraprabha, M.N.; Rangarajan, A.; Waiker, P.V.; Chidambara Murthy, K.N. Challenges in Healing Wound: Role of Complementary and Alternative Medicine. *Front. Nutr.* **2022**, *8*, 791899. [[CrossRef](#)]
3. Tiwari, R.; Pathak, K. Local Drug Delivery Strategies towards Wound Healing. *Pharmaceutics* **2023**, *15*, 634. [[CrossRef](#)]
4. Freedman, B.R.; Hwang, C.; Talbot, S.; Hibler, B.; Matoori, S.; Mooney, D.J. Breakthrough treatments for accelerated wound healing. *Sci. Adv.* **2023**, *9*, eade7007. [[CrossRef](#)] [[PubMed](#)]
5. Janoušková, O. Synthetic polymer scaffolds for soft tissue engineering. *Physiol. Res.* **2018**, *67*, S335–S348. [[CrossRef](#)] [[PubMed](#)]
6. Rahman, S.U.; Oh, J.-H.; Cho, Y.-D.; Chung, S.H.; Lee, G.; Baek, J.-H.; Ryoo, H.-M.; Woo, K.M. Fibrous topography-potentiating canonical Wnt signaling directs the odontoblastic differentiation of dental pulp-derived stem cells. *ACS Appl. Mater. Interfaces* **2018**, *10*, 17526–17541. [[CrossRef](#)]
7. Rahman, S.U.; Kim, W.-J.; Chung, S.H.; Woo, K.M. Nanofibrous topography-driven altered responsiveness to Wnt5a mediates the three-dimensional polarization of odontoblasts. *Mater. Today Bio* **2022**, *17*, 100479. [[CrossRef](#)]
8. Ma, Z.; Kotaki, M.; Inai, R.; Ramakrishna, S. Potential of nanofiber matrix as tissue-engineering scaffolds. *Tissue Eng.* **2005**, *11*, 101–109. [[CrossRef](#)] [[PubMed](#)]
9. Rahman, S.U.; Ponnusamy, S.; Nagrath, M.; Arany, P.R. Precision-engineered niche for directed differentiation of MSCs to lineage-restricted mineralized tissues. *J. Tissue Eng.* **2022**, *13*, 20417314211073934. [[CrossRef](#)] [[PubMed](#)]
10. Houschyar, K.S.; Duscher, D.; Rein, S.; Maan, Z.N.; Chelliah, M.P.; Cha, J.Y.; Weissenberg, K.; Siemers, F. Wnt Signaling During Cutaneous Wound Healing. In *Regenerative Medicine and Plastic Surgery: Skin and Soft Tissue, Bone, Cartilage, Muscle, Tendon and Nerves*; Duscher, D., Shiffman, M.A., Eds.; Springer International Publishing: Cham, Switzerland, 2019; pp. 147–155.
11. Whyte, J.L.; Smith, A.A.; Helms, J.A. Wnt signaling and injury repair. *Cold Spring Harb. Perspect. Biol.* **2012**, *4*, a008078. [[CrossRef](#)]
12. Subbukutti, V.; Sailatha, E.; Gunasekaran, S.; Manibalan, S.; Uma Devi, K.J.; Bhuvaneshwari, K.; Suvedha, R. Evaluation of wound healing active principles in the transdermal patch formulated with crude bio wastes and plant extracts against GSK-3 beta-an in silico study. *J. Biomol. Struct. Dyn.* **2023**, *41*, 1–12. [[CrossRef](#)] [[PubMed](#)]
13. Merrell, J.G.; McLaughlin, S.W.; Tie, L.; Laurencin, C.T.; Chen, A.F.; Nair, L.S. Curcumin-loaded poly(epsilon-caprolactone) nanofibres: Diabetic wound dressing with anti-oxidant and anti-inflammatory properties. *Clin. Exp. Pharmacol. Physiol.* **2009**, *36*, 1149–1156. [[CrossRef](#)] [[PubMed](#)]
14. Shishodia, S. Molecular mechanisms of curcumin action: Gene expression. *Biofactors* **2013**, *39*, 37–55. [[CrossRef](#)] [[PubMed](#)]
15. Panchatcharam, M.; Miriyala, S.; Gayathri, V.S.; Suguna, L. Curcumin improves wound healing by modulating collagen and decreasing reactive oxygen species. *Mol. Cell Biochem.* **2006**, *290*, 87–96. [[CrossRef](#)] [[PubMed](#)]
16. Xu, D.; Zhang, Y. Improving the physical realism and structural accuracy of protein models by a two-step atomic-level energy minimization. *Biophys. J.* **2011**, *101*, 2525–2534. [[CrossRef](#)]
17. Elumalai, M.; Muthaiah, R.; Alf, M.A. Identification of curcumin targets in neuroinflammatory pathways: Molecular docking scores with GSK-3 $\beta$ , p38 MAPK, COX, ICE and TACE enzymes. *Acta Pol. Pharm.* **2012**, *69*, 237–245.
18. Schneidman-Duhovny, D.; Inbar, Y.; Nussinov, R.; Wolfson, H.J. PatchDock and SymmDock: Servers for rigid and symmetric docking. *Nucleic Acids Res.* **2005**, *33*, W363–W367. [[CrossRef](#)]
19. Tabassum, N.; Khalid, S.; Ghafoor, S.; Woo, K.M.; Lee, E.H.; Samie, M.; Konain, K.; Ponnusamy, S.; Arany, P.; Rahman, S.U. Tideglusib-incorporated nanofibrous scaffolds potentially induce odontogenic differentiation. *J. Biomater. Appl.* **2023**, *38*, 280–291. [[CrossRef](#)]
20. Zhang, Q.; Oh, J.-H.; Park, C.H.; Baek, J.-H.; Ryoo, H.-M.; Woo, K.M. Effects of dimethyloxalylglycine-embedded poly( $\epsilon$ -caprolactone) fiber meshes on wound healing in diabetic rats. *ACS Appl. Mater. Interfaces* **2017**, *9*, 7950–7963. [[CrossRef](#)]
21. Bustanji, Y.; Taha, M.O.; Almasri, I.M.; Al-Ghoussein, M.A.; Mohammad, M.K.; Alkhatib, H.S. Inhibition of glycogen synthase kinase by curcumin: Investigation by simulated molecular docking and subsequent in vitro/in vivo evaluation. *J. Enzyme Inhib. Med. Chem.* **2009**, *24*, 771–778. [[CrossRef](#)]
22. Bainbridge, P. Wound healing and the role of fibroblasts. *J. Wound Care* **2013**, *22*, 407–408. [[CrossRef](#)] [[PubMed](#)]

23. Cianfruglia, L.; Minnelli, C.; Laudadio, E.; Scirè, A.; Armeni, T. Side effects of curcumin: Epigenetic and antiproliferative implications for normal dermal fibroblast and breast cancer cells. *Antioxidants* **2019**, *8*, 382. [[CrossRef](#)] [[PubMed](#)]
24. Ingavle, G.C.; Leach, J.K. Advancements in electrospinning of polymeric nanofibrous scaffolds for tissue engineering. *Tissue Eng. Part B Rev.* **2014**, *20*, 277–293. [[CrossRef](#)] [[PubMed](#)]
25. Perumal, G.; Pappuru, S.; Chakraborty, D.; Maya Nandkumar, A.; Chand, D.K.; Doble, M. Synthesis and characterization of curcumin loaded PLA-Hyperbranched polyglycerol electrospun blend for wound dressing applications. *Mater. Sci. Eng. C* **2017**, *76*, 1196–1204. [[CrossRef](#)]
26. Akhtar, M.; Woo, K.M.; Tahir, M.; Wu, W.; Elango, J.; Mirza, M.R.; Khan, M.; Shamim, S.; Arany, P.R.; Rahman, S.U. Enhancing osteoblast differentiation through small molecule-incorporated engineered nanofibrous scaffold. *Clin. Oral Investig.* **2022**, *26*, 2607–2618. [[CrossRef](#)] [[PubMed](#)]
27. Prudovsky, I. Cellular Mechanisms of FGF-Stimulated Tissue Repair. *Cells* **2021**, *10*, 1830. [[CrossRef](#)]
28. Akita, S.; Akino, K.; Hirano, A. Basic Fibroblast Growth Factor in Scarless Wound Healing. *Adv. Wound Care* **2013**, *2*, 44–49. [[CrossRef](#)]
29. Shishodia, S.; Sethi, G.; Aggarwal, B.B. Curcumin: Getting back to the roots. *Ann. N. Y. Acad. Sci.* **2005**, *1056*, 206–217. [[CrossRef](#)]
30. Mansouri, K.; Rasoulpoor, S.; Daneshkhah, A.; Abolfathi, S.; Salari, N.; Mohammadi, M.; Rasoulpoor, S.; Shabani, S. Clinical effects of curcumin in enhancing cancer therapy: A systematic review. *BMC Cancer* **2020**, *20*, 791. [[CrossRef](#)]
31. Anand, P.; Sundaram, C.; Jhurani, S.; Kunnumakkara, A.B.; Aggarwal, B.B. Curcumin and cancer: An “old-age” disease with an “age-old” solution. *Cancer Lett.* **2008**, *267*, 133–164. [[CrossRef](#)]
32. Miguel, S.P.; Sequeira, R.S.; Moreira, A.F.; Cabral, C.S.; Mendonça, A.G.; Ferreira, P.; Correia, I.J. An overview of electrospun membranes loaded with bioactive molecules for improving the wound healing process. *Eur. J. Pharm. Biopharm.* **2019**, *139*, 1–22. [[CrossRef](#)] [[PubMed](#)]
33. Koike, Y.; Yozaki, M.; Utani, A.; Murota, H. Fibroblast growth factor 2 accelerates the epithelial–mesenchymal transition in keratinocytes during wound healing process. *Sci. Rep.* **2020**, *10*, 18545. [[CrossRef](#)] [[PubMed](#)]
34. Wang, X.; Zhu, Y.; Sun, C.; Wang, T.; Shen, Y.; Cai, W.; Sun, J.; Chi, L.; Wang, H.; Song, N. Feedback activation of basic fibroblast growth factor signaling via the Wnt/ $\beta$ -catenin pathway in skin fibroblasts. *Front. Pharmacol.* **2017**, *8*, 32. [[CrossRef](#)]
35. Zubair, M.; Ahmad, J. Role of growth factors and cytokines in diabetic foot ulcer healing: A detailed review. *Rev. Endocr. Metab. Disord.* **2019**, *20*, 207–217. [[CrossRef](#)]
36. Nicolas, J.; Magli, S.; Rabbachin, L.; Sampaolesi, S.; Nicotra, F.; Russo, L. 3D Extracellular Matrix Mimics: Fundamental Concepts and Role of Materials Chemistry to Influence Stem Cell Fate. *Biomacromolecules* **2020**, *21*, 1968–1994. [[CrossRef](#)]
37. Schlie-Wolter, S.; Ngezahayo, A.; Chichkov, B.N. The selective role of ECM components on cell adhesion, morphology, proliferation and communication in vitro. *Exp. Cell Res.* **2013**, *319*, 1553–1561. [[CrossRef](#)] [[PubMed](#)]
38. Situm, M.; Kolić, M. Chronic wounds: Differential diagnosis. *Acta Med. Croatica* **2013**, *67* (Suppl. S1), 11–20.
39. Sidhu, G.S.; Singh, A.K.; Thaloor, D.; Banaudha, K.K.; Patnaik, G.K.; Srimal, R.C.; Maheshwari, R.K. Enhancement of wound healing by curcumin in animals. *Wound Repair Regen.* **1998**, *6*, 167–177. [[CrossRef](#)] [[PubMed](#)]
40. Mohanty, C.; Sahoo, S.K. The in vitro stability and in vivo pharmacokinetics of curcumin prepared as an aqueous nanoparticulate formulation. *Biomaterials* **2010**, *31*, 6597–6611. [[CrossRef](#)] [[PubMed](#)]

**Disclaimer/Publisher’s Note:** The statements, opinions and data contained in all publications are solely those of the individual author(s) and contributor(s) and not of MDPI and/or the editor(s). MDPI and/or the editor(s) disclaim responsibility for any injury to people or property resulting from any ideas, methods, instructions or products referred to in the content.